MAGNETIC PROPERTIES OF SELECTED SPACECRAFT MATERIALS

P. W. Droll[1] and E. J. Iufer[1]

REFERENCE: P. W. Droll and E. J. Iufer, "Magnetic Properties of Selected Spacecraft Materials," University of Nevada and Ames Research Center, NASA, Cosponsored Symposium on Space Magnetic Exploration and Technology (August 1967).

ABSTRACT: This paper summarizes the results of an investigation of the magnetic properties of selected spacecraft materials. Experimental measurements describing the effects of magnetic field exposure, shock, vibration, and temperature on the induced and remanent dipole moment of Kovar, Dumet, Invar, Nickel, 304SS, 410SS, and 416SS rod specimens are presented. Analysis of the data indicates that temperatures of 77° K to 390° K, shock to 50 g, and vibration to 25 g produce negligible effects on dipole moment for specimens having length-to-diameter ratios of 5.5. The remanent and induced moments of rod samples having length-to-diameter ratios of 40 or less are linearly related to magnetizing forces less than 25 oersteds. By means of the data provided, predictions of the dipole moment can be made for these materials if the alloy, demagnetization factor, magnetizing field, volume, and length-to-diameter ratio are known.

Nomenclature

B	magnetic induction (B_r, residual induction; B_{rs}, retentivity; B_s, saturation induction)
D	diameter
H	magnetizing force, magnetic field strength (H_a, applied field; H_c, coercive force; H_{cs}, coercivity)
I	intensity of magnetization
L	length
M	magnetic moment
m	length to diameter ratio
N	demagnetizing factor
R	measurement range
V	volume
μ	permeability, normal
μ'	permeability, apparent

[1]Research Scientist, Ames Research Center, NASA, Moffett Field, California 94035.

Introduction

Recent emphasis on the systematic exploration of the boundary of the Earth's magnetosphere and beyond has served to set strict limitations on the magnitude of magnetic fields produced by the spacecraft. To assure that spacecraft fields do not degrade the accuracy of the flight magnetometers, maximum field intensities of 1 nanotesla (1 gamma) are being specified for the complete spacecraft. This specification is related to current flight magnetometer sensitivity of 0.1 nanotesla and the 4 to 10 nanotesla quiescent level of the interplanetary magnetic field. As listed in Table 1, the fields of previously flown spacecraft (1), which were of sufficient interest to be reported, range from approximately 0.2 to 58.8 nanotesla at a range of 2 meters (nominal sensor location). Design of spacecraft complying with 1 nanotesla, or less, require close attention to the magnetic properties of all materials used in fabrication.

Although achievement of a low-moment spacecraft design would be realized by elimination of all ferromagnetic materials, a large percentage of electronic parts still contain magnetic materials. Therefore, it is extremely useful to know the magnetic properties of these essential components to provide a basis for design and prediction of spacecraft fields.

Much information on the types of materials used in the design of conventional magnetic circuits may be found in the literature. The magnetic properties of the materials studied in this report are incidental to their application, and consequently, little or no information can be found on their pertinent magnetic properties. Experimental measurements have been made to provide the missing information under conditions simulating the environmental exposures occurring during the manufacture, transportation, and launch of spacecraft.

By means of the Tables and Curves found in this report, it is possible to make estimates of the magnetic moments of spacecraft components.

Basic Relationships in Ferromagnetism

There are two basic magnetic quantities and an arbitrary constant from which all other magnetic quantities are derived (2). They are magnetic induction, B, magnetizing force, H, and permeability, μ_o. Magnetic induction is the quantity measured by the mechanical force experienced by a current-carrying conductor in a magnetic field. The measure of the ability of an electric current to produce magnetic induction at a given point is called the magnetizing force, H. Permeability is the ratio of the magnetic induction to the

corresponding magnetizing force. The value assigned to the permeability of free space, μ_o, determines the system of units and is equal to $4\pi \times 10^{-7}$ henries per meter in the MKS system and to unity in the c.g.s.-e.m.u. system used in this report.

With the definitions of B, H, and μ, a dynamic set of characteristics may be defined. If a demagnetized closed ring specimen is subjected to increasing values of H, there is a corresponding but nonlinear increase in B. This effect is illustrated in Fig. 1, and is called the normal induction or virgin magnetization curve. The hysteresis of the material is characterized by the partial retention of the induction when H is reduced to zero. If the material were previously magnetized to saturation, the induction retained is called the retentivity, B_{rs}; for lower exposure levels, the term residual induction B_r is used. The negative magnetizing force at which B_r becomes zero is called the coercive force, H_c, and the moment at which B_{rs} becomes zero is called the coercivity, H_{cs}.

Magnetic induction is made up of two components: one induced in the space occupied by the specimen (H) and the other due to the intrinsic magnetization of the specimen ($4\pi I$). That is

$$\bar{B} = \bar{H} + 4\pi\bar{I}$$

or

$$\bar{I} = \frac{\bar{B} - \bar{H}}{4\pi} \qquad (1)$$

and $\bar{I}$ is the intensity of magnetization (3). Equation (1) is sometimes called the magnetic equation of state because it describes the behavior of ferromagnetic media in a magnetic field.

These equations assume homogeneity in the magnetic circuit typified by torroidal core structures. However, spacecraft, magnetic material shapes can often be approximated by slender cylinders. The relatively high reluctance of space as compared to that of the material causes the net magnetizing force inside the rod to be less than the applied field. Classically this dimunition is attributed to the formation of fictitious poles at the ends of the rod. As a result, the hysteresis curve for the rod specimen appears to be sheared in comparison with the hysteresis curve of closed rings as shown in Fig. 1.

For rod specimens (4) the equation of state is

$$\bar{H} = \bar{H}_o - N\bar{I}$$

or the equivalent

$$\bar{H} = \bar{H}_o - N\left(\frac{\bar{B} - \bar{H}}{4\pi}\right) \qquad (2)$$

Where $\bar{H}$ is the magnetizing field acting on the middle of the rod, $\bar{H}_o$ the applied field equal to that which would exist if the specimen were removed and $\bar{B}$ the flux density measured at the middle of the rod. N represents the demagnetizing factor to accommodate for specimen shape with a finite length to diameter ratio (m). It is assumed that $\bar{H}$, $\bar{B}$, and $\bar{I}$ are parallel to $\bar{H}_o$ and uniform throughout the specimen, which permits the vector notation to be discarded.

The normal permeability of a ferromagnetic material is defined as $\mu = B/H$ measured on a closed loop specimen. The magnetic induction is measured for known values of H, and μ is calculated. For a cylindrical specimen made from the same material the effective permeability (μ') is less and may be defined by

$$\mu' = \frac{B}{H_o} \qquad (3)$$

Substituting (3) and the definition of normal permeability into equation (2) yields

$$\frac{1}{\mu - 1} = \frac{\mu}{\mu'(\mu - 1)} - \frac{N}{4\pi} \qquad (4)$$

If $\mu \gg 1$

$$\frac{1}{\mu} = \frac{1}{\mu'} - \frac{N}{4\pi}$$

For known values of H_o, N, and μ the induction B may be calculated from equation (3). Substituting equation (4) into (2) yields

$$H = \frac{H_o[1 + (N/4\pi)] - (NB/4\pi)}{1 - (N/4\pi)} \qquad (5)$$

The intensity of magnetization is obtained by substituting (5) into (1) and

$$I = \frac{1}{4\pi}\left\{B - \frac{H_o[1 + (N/4\pi)] - (NB/4\pi)}{1 - (N/4\pi)}\right\}$$

The magnetic moment, M, of a body is equal to the volume integral of the vector, I, and for rods, assuming M is parallel to L is

$$M = IV$$

After calculating the magnetic moment of the rod, the magnetic fields can be calculated at any range using the dipole approximation. The on axis field of a magnetic dipole is given by

$$H = \frac{2M}{R^3}$$

where R is the distance from the geometric center of the specimen to the point of measurement. Therefore, the external magnetic field produced by cylindrical shaped specimens can be calculated if the permeability, magnetizing force, and the length-to-diameter ratio is known. However, because of the simplifying assumptions, experimental measurements are relied upon to determine the curve relating permeability to the intensity of magnetization and to find the curves for residual induction and coercive force.

Materials Selection

Seven ferromagnetic materials commonly used for spacecraft electronic or structural purposes were selected for this study. These materials and their uses are listed in Table 2. The purity and some properties of these materials, shown in Table 3, were verified by independent measurement. The geometrical shapes of the specimens studied are listed in Table 4.

Experimental Apparatus

The magnetic field measurements of the specimens were made in the Ames Research Center 12-foot coil facility (5). The Earth's magnetic field was canceled to eliminate induced moments in the specimens during residual induction measurements. High field

intensities were generated using a multiturn coil approximately 10 cm long and 10 cm in diameter which produced fields from zero to 400 gauss uniform to ±3% over the volume of the specimens. The low field intensities were generated using a solenoid 61 cm in length and having a bore approximately 15 cm in diameter. The magnetic field intensities of the specimens were measured with a fluxgate magnetometer[2] sensitive to 0.2 gamma.

Experimental Procedure

Induction Measurement

The magnetic induction tests were performed on demagnetized specimens. The stray fields of the coil were compensated using circuitry built into the magnetometer. After placing the specimens in the unenergized coil, the current was adjusted to provide a preselected magnetizing force and the resulting field intensity measured by the magnetometer was recorded. The specimen was then withdrawn and demagnetized in preparation for the next higher exposure level.

Residual Induction Measurements

The procedures used for the residual magnetic induction measurements were similar to the tests for magnetic induction. The depermed specimens were placed in the coil and exposed to a known magnetizing force. After the coil was de-energized, the residual magnetic fields of the specimens were measured using the magnetometer under zero ambient field conditions.

Coercive Force Measurements

Coercive force measurements were made after each specimen had been exposed to a known magnetizing force. The residual magnetic induction was brought to zero by applying a momentary magnetizing force in the direction opposite to the initial exposure. Values for the initial exposure and for the reversed exposure which reduced the residual induction to zero were recorded. Conventional coercive force measurements are made during application of a magnetizing force which reduces the induction to zero. However, for these studies, momentary exposures were used to realistically simulate the exposures received by spacecraft.

Vibration and Shock Effects Measurements

Vibration stresses were induced into the specimens using a M.B. Electronics Model 2750MB amplifier with a Model C11-D calibrator/exciter system. The accelerometer used to monitor the g levels was a Columbia Model 504-3 with a Model 602 Dial-A-Gail amplifier. The drive unit was set up at a remote location to avoid magnetic interference. A nylon shaker fixture which held the specimens was connected horizontally to the exciter system via a 182 cm (6 ft) thin-walled aluminum push rod, 1.5 cm in diameter. Dead load deflection of the push rod was reduced by use of a two point suspension near its center. The natural resonant frequency of the rod and fixture was determined to be outside the vibration frequency band of interest. An acceleration level of 25 g was induced in the samples over a frequency range of from zero to 2000 Hertz for a period of time not exceeding 300 seconds to simulate the launch environment. The specimens were first vibrated while in a 25 oersted magnetizing force to determine the induced moment effects and then vibrated after a momentary exposure to a 25 oersted magnetizing force to determine residual moment effects.

The specimens were subjected to shock stresses by dropping the specimens on a hard surface from an elevation of approximately 30 cm to obtain a shock level of approximately 50 g. Shock tests were performed on the specimens after they were subjected to a magnetizing force of 25 oersted to determine if the residual magnetic induction would change.

Temperature Effects Measurements

The influence of temperature on B_r stability was determined by exposing specimens to a 100 gauss magnetizing force and then varying the temperature. Measurements of the magnetic field intensity were performed on specimens at 390° K and 77° K.

Error Analysis

The estimated error in the calculated induction field values is $\leq 100\%$. The error is attributed to the following: (a) variations in properties resulting from composition or processing and (b) nonuniform magnetization intensity over the entire cylindrical shape. The estimated uncertainty of the calculated values of magnetic moment obtained from measurements of the external field is considered to be less than 5% including random and systematic errors.

Temperature measurement uncertainties of 15° K at the elevated temperature and 3° K at the low temperature resulted primarily from the inability to attach thermocouples directly to the specimens.

Experimental Results

The materials tested can be divided into two types according to application: The first type, consisting of Kovar, Invar, Dumet, and Nickel, is used in the manufacture of electronic parts and is presented together in the graphs. The second type, consisting of 416, 410, and 304 stainless steel, is used in the manufacture of structures and fasteners and is similarly grouped.

Induction Properties

The induction moments of seven different materials were obtained for various length to diameter ratios as a function of magnetizing force. Also, the induction moment of Kovar was measured as a function of length to diameter ratio at one level of magnetizing force.

The induction moments of Kovar, Invar, and Dumet are shown in Fig. 2. The Kovar and Invar samples, tested in configuration A (m = 5.5) exhibit a very linear response to magnetizing forces less than 100 oersteds. However, the Kovar and Dumet samples in configuration B (m = 40), show a tendency to saturate at the 100 oersted level. The test results on the 416SS, 410SS, 304SS, and Nickel samples in configuration A did not tend to saturate

[2]Forster-Hoover M. F. 5050

as the magnetizing force approached the 100 oersted level. Figure 3 illustrates typical data as a function of magnetizing force. The 410SS and 416SS data are plotted as one curve because their characteristics are very similar, see Table 2.

The effect of m on the induced moment of Kovar samples tested in configurations B through L at a magnetizing force level of 1 oersted is shown in Fig. 4, and listed in Table 13. The low level of magnetizing force was chosen to assure that the specimen would not saturate in configuration L (m = 240). However, the theoretical induced moment curve does show a tendency to saturation at high m values. The results of this test illustrate a very important design consideration. That is, if a long piece of magnetic lead material were reduced in length, by an order of magnitude, the induced moment of the lead would be diminished by approximately two orders of magnitude. Reducing the m value is then an effective method of reducing induced moment.

Residual Induction Properties

The residual induction moments of all the materials are shown in Figs. 5 and 6, and listed in Tables 5 through 12. The results shown in Fig. 5 indicate that the residual induced moment of Kovar and Dumet with high values of m(40) approach saturation at relatively low levels of magnetizing force. In fact, it could be inferred that they will saturate very close to the 30 oersted level. It appears that the knee of the Dumet curve is closer to the 20 oersted level. The Kovar and Invar samples with m's of 5.5 show linear characteristics over the magnetizing force range with only slight tendencies to saturate. Curves similar in shape to the Kovar and Invar, m = 5.5, were obtained for Nickel, 416SS and 410SS as shown in Fig. 6. A general comparison of Figs. 5 and 6 indicate that all of the materials except 304SS are equally magnetic. Since 304SS is an austenitic stainless, it should exhibit lower magnetizations.

Coercive Force Properties

The coercive force properties of all the configuration A materials except Dumet, were obtained as a function of magnetizing force. These results are shown in Fig. 7. The data illustrate that 304SS is the only material exhibiting a linear response to magnetizing force over the range of zero to 100 oersteds. That is, a fixed percentage of the magnetizing force, if applied in the opposite direction in the sample will always reduce the residual induction to a zero value. It should be noted that a similar condition exists for the other materials at magnetizing forces less than approximately 25 oersteds.

Vibration and Shock Effects on Properties

The vibration and shock levels which were determined from known levels of the THOR DELTA launch environment, were induced into the specimens in configuration A. The specimens were subjected to vibration levels while in a magnetizing field of 25 oersteds and again in zero ambient field after momentary exposure at the same level. They were subjected to shock stresses on the order of 50 g after a momentary exposure of 25 oersteds. The results of those tests indicate that mechanical effects on the magnetic properties of specimens with m = 5.5 are negligible (less than 5%) for magnetizing fields of 25 oersteds.

Temperature Effects on Properties

The samples in configuration A were subjected to temperatures of 390° K and 77° K after exposure to a 25 oersted magnetizing force. Data obtained with specimens at these temperatures showed a negligible change.

Discussion

Comparisons of experimental data with values of induction moment calculated for Kovar (6), Invar (7), Nickel (8), 416SS (8), are shown in Figs. 2 and 3.

Reasonably good agreement is shown for all specimens at the high levels of magnetizing force because the permeability is becoming more nearly constant. Better agreement could be obtained if equation (3) were expanded to account for the nonuniform intensity of magnetization in cylindrical specimens. A closer approximation to B might be obtained by integrating B over the length of the rod to find some average value correction factor. Bozarth (3) suggests the need for "some kind of averaging." The figures indicate that the experimental and theoretical values agree within a factor which ranges from about 1.2 to 2.

No theoretical model was found which would permit accurate calculation of the residual induction moment as a function of magnetizing force. An attempt was made to apply a hyperbolic demagnetization curve approximation based on permanent magnet materials to these specimens; however, the development proved invalid. In lieu of a mathematical model, one can use the residual induction moment data contained in this report for estimating the residual moment of parts. Recalling that the induction B is always larger than the B_r, for a given exposure level, one may calculate a worst case remanent moment using the equations for induction.

Conclusions

An analytical model of the induction moment of rod specimens, based on formulas available in the literature, was derived. Experimental verification of the model was accomplished by demonstrating the influence of permeability, demagnetization factor, magnetizing force, and volume on the materials. The model was found to give a reasonably accurate prediction of induction moment for specimens whose length to diameter ratio ranged from 5 to 100. Analysis of the induction moment experimental data indicates the following:

The calculated value of induction moment was always larger than the experimental value.

All of the controlled expansion alloys studied have similar magnetic properties and their induction moments are approximately linear for magnetizing environments less than 30 gauss.

The magnetic moment of a cylindrical specimen can decrease two orders of magnitude for a decrease in length to diameter ratio of one order of magnitude.

Efforts to develop an analytical model for calculating the coercive force and the residual induction

moment were not successful. The experimental measurements covering the length-to-diameter ratios and the magnetic field exposure levels of interest in spacecraft design support certain generalizations: For any one material, the residual induction moments are at least an order of magnitude less than the induction moments for a given magnetizing force. The residual induction moment may be linearly extrapolated to low field values for magnetizing forces less than 25 gauss. For probable spacecraft exposure field levels (1-10 gauss), there is little basis for distinguishing between the controlled expansion alloys on the basis of their residual induction moments.

The coercive force measurement data indicate that all of materials tested with a length to diameter ratio of 5.5 are similar in their response to magnetizing forces of less than 10 gauss. In addition, the ratio of the coercive force to the magnetizing force tends to be a constant value of approximately 0.5 for the 10 gauss field level.

From the standpoint of material selection, there is apparently no basis for selecting Dumet in preference to Kovar from a magnetic moment standpoint.

The use of linear extrapolation techniques to estimate residual induction moment of specimens having length-to-diameter ratios in the order of five is apparently valid for standard exposure fields of 25 gauss or less.

References

1. C. L. Parsons, "Magnetic Testing of Spacecraft," Proceedings of the Magnetics Workshop, compiled by J. G. Bastow, Jet Propulsion Laboratory, TM 33-216, September 15, 1965.

2. R. L. Sanford, and I. L. Cooter, "Basic Magnetic Quantities and the Measurement of the Magnetic Properties of Materials." National Bureau of Standards Monograph 47, May 1962.

3. R. M. Bozarth, "Ferromagnetism," D. Van Nostrand Company, Inc., p. 3, 1951.

4. R. M. Bozarth, and D. M. Chopin, "Demagnetizing Factors for Rods," J. Appl. Phys., vol. 13, pp. 320-326, May 1942.

5. E. J. Iufer, and P. W. Droll, "Space Magnetic Environment Simulation for Spacecraft Testing," to be presented at ASTM/IES/AIAA Second Space Simulation Conference (September 1967), Am. Soc. Testing Mats., 1967.

6. "Kovar Expansion Alloy," Application Data Sheet 52-461, Westinghouse Electric Corporation, Los Angeles, California, May 1965.

7. "Carpenter Alloys for Electronic, Magnetic and Electrical Applications," The Carpenter Steel Company, Reading, Pennsylvania, 1963.

8. "Electrical Materials Handbook," Allegheny Ludlum Steel Corporation, Pittsburgh 22, Pennsylvania, 1961.

TABLE 1--Magnetic fields of some interplanetary spacecraft.

Spacecraft	Date	Post 25 gauss[a] magnetizing force	Demagnetized[a]
OGO-A (8)	4/15/64	146.8	58.8
Explorer (8) IMP-C	7/30/64	15.7	0.6
Explorer XXI (8) IMP-B	8/14/64	12.3	0.5
Pioneer VI	12/16/65	1.6	0.2
Pioneer VII	8/17/66	1.5	0.2

[a]Approximate measurement range, 2 meters.

TABLE 2--Materials selected for study.

Materials	Use	Comment
Nickel	Electronic components	A standard lead material; good weldability
Kovar	Electronic components	Controlled expansion alloy; useful lead material - has coefficient of thermal expansion matching glass
Dumet	Electronic components	Standard lead material, good weldability
Invar	Electronic components	Controlled expansion alloy
410 stainless steel	Structural	General purpose stainless steel. Excellent availability; good resistance to chemicals and atmosphere
416 stainless steel	Structural	Free machining modification of type 410
304 stainless steel	Structural	Low carbon modification of 302SS. Excellent atmosphere resistance and machinability

TABLE 3--Chemical and physical properties of rod specimens.

Material	Source	Major constituents, %									Rockwell hardness		Comment
		C	Cr	Fe	Mn	Ni	P	Si	S	Co	B	C	
Nickel	Pacific Metals	0.03	---	---	---	PC*	---	0.08	---		90.5		Cold drawn heat #N7050A
Kovar	Westinghouse Electric Co.	---	---	53.00	0.46	29.00	---	0.01	---	17.53	82.8		Heat #920050
Dumet	General Electric Company	---	---	57.00	1.00	42.00	---	---	---	---	---		Has copper sheath
Invar	Carpenter steel	0.08	---	PC	0.87	35.74	---	0.31	---	---	94.0		Cold drawn heat #66719
410SS	Carpenter steel	0.12	12.13	PC	0.53	---	0.01	0.33	0.01	---	98.5		Cold drawn heat #810491
416SS	Ames Research Center Stock item	0.01	12.85	PC	0.82	---	0.02	0.36	0.26	---	98.5		Annealed grain size ASTM #9
304SS	Carpenter steel	0.07	18.30	PC	0.94	8.47	0.03	0.64	0.02	---		28.5	Cold drawn heat #67844

*Principal constituent - remainder of percentage.

TABLE 4--Geometrical properties of rod specimens.

Configuration	Length, cm	Diameter, cm	Volume, cubic cm	M
A	5.080	0.952	3.62	5.47
B	5.080	0.127	0.06	40.00
C	7.62	0.127	0.10	60.00
D	10.16	0.127	0.13	80.00
E	12.70	0.127	0.16	100.00
F	15.24	0.127	0.19	120.00
G	17.78	0.127	0.22	140.00
H	20.32	0.127	0.26	160.00
I	22.86	0.127	0.29	180.00
J	25.40	0.127	0.32	200.00
K	27.94	0.127	0.35	220.00
L	3048	0.127	0.38	240.00

TABLE 5--Results of nickel tests.
[$N/4\pi = 0.036$, $m = 5.4$, $V = 3.621$ cm]

Magnetizing force, oersted	Normal permeability	Field intensity, theoretical, gamma	Field intensity, experimental, gamma	Induction moment, theoretical, gauss-cm^3	Induction moment, experimental, gauss-cm^3	Residual induction moment, experimental, gauss-cm^3	Coercive force, experimental, oersted
0.5	*	---	14.7	---	2.08	---	---
1.0	1000	54.9	27.8	7.8	3.9	0.0	---
5.0	720	271.8	124.0	38.5	17.6	0.2	2.3
10.0	410	528.1	280.0	74.8	39.6	0.7	---
15.0	287	770.4	420.0	109.1	59.5	1.8	7.5
20.0	220	999.2	568.0	141.5	80.4	3.3	---
25.0	180	1217.3	717.0	172.4	101.5	5.2	12.9
35.0	---	---	---	---	---	10.8	18.2
100.0	58	3754.2	3313.0	531.5	469.1	75.0	42.1

*Data unavailable.

TABLE 6--Results of Kovar tests.
[$N/4\pi$ = 0.036, m = 5.4, V = 3.6 cm^3, R = 30.48 cm]

Magnetizing force, oersted	Normal permeability	Field intensity, theoretical, gamma	Field intensity, experimental, gamma	Induction moment, theoretical, gauss-cm^3	Induction moment, experimental, gauss-cm^3	Residual induction moment, experimental, gauss-cm^3	Coercive force, experimental, oersted
0.5	1000	27.4	20.6	3.9	2.9	---	---
1.0	2000	55.7	39.0	7.9	5.5	0.0	---
5.0	2375	279.3	193.0	39.5	27.3	0.2	2.3
10.0	1600	555.3	388.0	78.6	54.9	0.8	---
15.0	1300	829.6	580.0	117.4	82.1	1.8	7.1
20.0	1100	1101.8	769.0	155.9	108.9	2.9	---
25.0	900	1369.4	946.0	193.8	133.9	4.2	10.9
35.0	---	---	---	---	---	6.6	14.2
100.0	200	4938.1	4330.0	699.2	613.1	18.1	26.1

TABLE 7--Results of Kovar tests.
[$N/4\pi$ = 0.0018, m = 40, V = 0.064 cm]

0.5	1000	6.4	3.8	0.9	0.5	---	---
1.0	2000	15.7	7.6	2.2	1.1	0.0	---
5.0	2375	81.2	47.5	11.5	6.7	1.3	---
10.0	1600	148.7	88.0	21.0	12.4	2.3	---
15.0	1300	210.5	140.0	29.8	19.8	3.0	---
20.0	1100	266.1	176.0	37.7	24.9	3.6	---
25.0	900	309.5	210.0	43.8	29.7	3.8	---
35.0	---	---	---	---	---	4.1	---
100.0	200	527.9	434	74.7	61.4	4.3	---

TABLE 8--Results of Dumet tests.
[$N/4\pi$ = 0.0018, m = 40, V = 0.064 cm^3, R = 30.48 cm]

0.5	*	---	2.7	---	0.4	---	---
1.0	*	---	5.1	---	0.7	0.0	---
5.0	*	---	30.0	---	4.2	0.8	---
10.0	*	---	68.0	---	9.6	3.0	---
15.0	*	---	98.5	---	13.9	5.1	---
20.0	*	---	134.0	---	18.9	6.6	---
25.0	*	---	163.0	---	23.1	7.6	---
35.0	*	---	---	---	---	8.1	---
100.0	*	---	370.0	---	52.4	9.8	---

TABLE 9--Results of Invar tests.
[$N/4\pi$ = 0.036, m = 5.4, V = 3.6 cm^3, R = 30.48 cm]

0.5	*	---	21.2	---	3.0	---	---
1.0	85	42.1	40.0	6.0	5.7	0.0	---
5.0	500	267.2	203.0	37.8	28.7	0.3	2.6
10.0	610	539.8	411.0	76.4	58.2	1.3	---
15.0	470†	798.5	618.0	113.0	87.5	2.9	8.0
20.0	400†	1054.5	824.0	149.3	116.7	4.8	---
25.0	300†	1289.1	1006.0	182.5	142.4	6.5	10.3
35.0	*	---	---	---	---	9.3	12.3
100.0	*	---	4135.0	---	585.4	19.4	21.0

*Data unavailable.
†Extrapolated.

TABLE 10--Results of 416SS tests.
[$N/4\pi$ = 0.036, m = 5.4, V = 3.6 cm^3, R = 30.48 cm]

Magnetizing force, oersted	Normal permeability	Field intensity, theoretical, gamma	Field intensity, experimental, gamma	Induction moment, theoretical, gauss-cm^3	Induction moment, experimental, gauss-cm^3	Residual induction moment, experimental, gauss-cm^3	Coercive force, experimental, oersted
0.5	*	---	19.8	---	2.8	---	---
1.0	500	50.3	36.8	7.6	5.2	0.0	---
5.0	600	269.7	196.0	38.2	27.7	0.3	2.3
10.0	760	544.6	394.0	77.1	55.8	1.1	---
15.0	647	811.8	592.0	114.9	83.8	2.3	6.8
20.0	550	1074.3	785.0	152.1	111.1	3.7	---
25.0	465	1330.5	964.0	188.4	136.5	5.3	11.7
35.0	---	---	---	---	---	8.6	14.0
100.0	160	4785.8	4090.0	677.6	579.1	27.3	30.0

TABLE 11--Results of 410SS tests.
[$N/4\pi$ = 0.036, m = 5.4, V = 3.6 cm^3, R = 30.48 cm]

0.5	*	---	19.8	---	2.8	---	---
1.0	500	50.3	36.8	7.6	5.2	0.0	---
5.0	600	269.7	196.0	38.2	27.2	0.3	2.3
10.0	760	544.6	394.0	77.1	55.8	1.1	---
15.0	647	811.8	592.0	114.9	83.8	2.3	6.7
20.0	550	1074.3	785.0	152.1	111.1	3.7	---
25.0	---	1330.5	964.0	188.4	136.5	5.3	11.9
35.0	---	---	---	---	---	8.7	14.1
100.0	160	4785.8	4090.0	677.6	579.1	27.2	29.9

TABLE 12--Results of 303SS tests.
[$N/4\pi$ = 0.036, m = 5.4, V = 3.62 cm^3, R = 30.48 cm]

0.5	*	---	0.5	---	0.1	---	---
1.0	*	---	0.8	---	0.1	0.0	0.0
5.0	*	---	3.0	---	0.4	0.0	3.0
10.0	*	---	6.6	---	0.9	0.0	---
15.0	*	---	10.2	---	1.4	0.0	9.0
20.0	*	---	13.5	---	1.9	0.0	---
25.0	*	---	16.2	---	2.3	0.1	15
35.0	*	---	---	---	---	0.2	20
100.0	*	---	80.0	---	11.3	3.1	59.1

*Data unavailable.

TABLE 13--Theoretical and experimental induction moments of Kovar as a function of L/D ratio H_o = 1 oersted, μ = 2000.

(L/D) m	$N/4\pi \times 10^{-5}$	Volume, cm^3	Measurement, range-cm	Field intensity, theoretical, gamma	Field intensity, experimental, gamma	Induction moment, theoretical, gauss-cm^3	Induction moment, experimental, gauss-cm^3
240	6.2	0.385	152.4	3.1	1.7	54.6	30.1
220	7.4	0.353	139.7	3.6	2.0	48.9	27.2
200	9.0	0.321	127.0	4.2	2.0	43.3	20.5
180	11.0	0.289	114.3	5.0	2.6	37.7	19.4
160	14.0	0.257	101.6	6.1	3.0	31.9	15.7
140	18.0	0.225	88.9	7.5	4.7	26.3	16.5
120	25.0	0.193	76.2	9.2	6.3	20.4	13.9
100	36.0	0.161	63.5	11.6	9.1	14.8	11.6
80	54.0	0.129	50.8	15.0	11.2	9.8	7.3
60	90.0	0.096	38.1	19.7	20.0	5.4	5.5
40	180.0	0.064	25.4	27.1	---	2.2	---

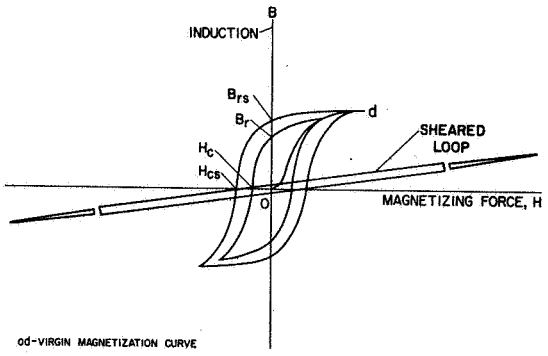

Fig. 1--Normal and sheared hysteresis loops.

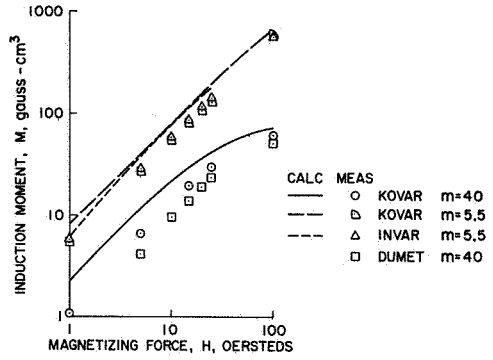

Fig. 2--Effect of magnetizing force on induction moment.

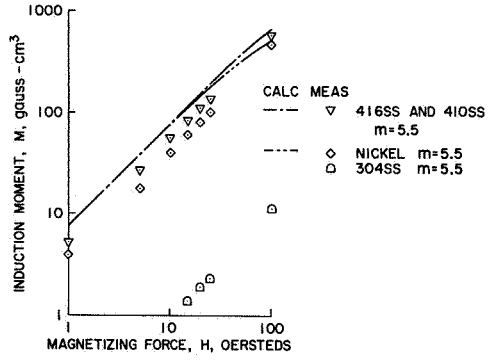

Fig. 3--Effect of magnetizing force on induction moment.

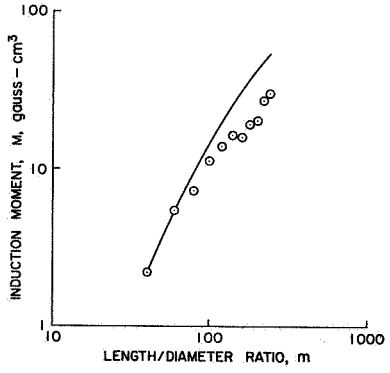

Fig. 4--The effect of length-to-diameter ratio on induction moment for Kovar.

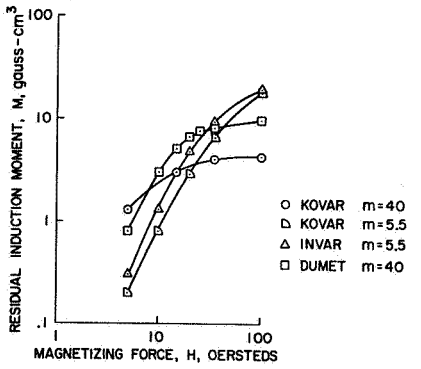

Fig. 5--Effect of magnetizing force on residual induction moment.

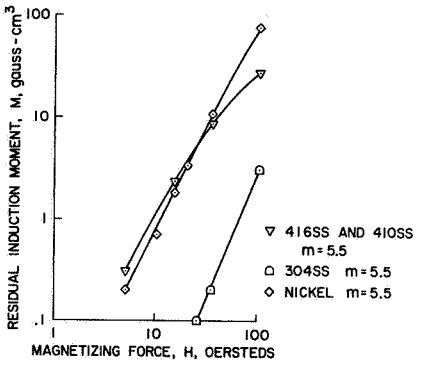

Fig. 6--Effect of magnetizing force on residual induction moment.

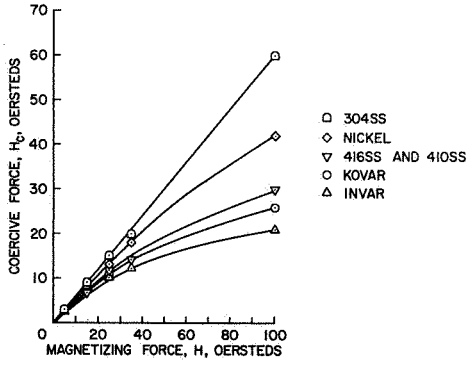

Fig. 7--Effect of magnetizing force on coercive force.